DOI: 10.1002/chem.200902859

Design and Preparation of Co-crystals Utilizing the $R^2_4(8)$ Hydrogen-Bonding Motif

Joel Bernstein,*[a] Juan J. Novoa,[b] Roland Boese,[c] and Sebastian A. Cirkel[c]

Abstract: An investigation of the feasibility of utilizing a specific, and previously largely unrecognized, hydrogen-bonded synthon for the design and preparation of co-crystals is reported. Structural evidence (i.e., >12000 instances) indicated the robustness of the cyclic $R^2_4(8)$ hydrogen-bonded motif containing, in most cases, four individual (either identical or different) molecules, in which the donor substituent (e.g., an amine) can provide two hydrogen-bond donors, and the acceptor (e.g., a carbonyl oxygen) can provide two hydrogen-bond acceptors. The energetic robustness of the motif with respect to chemical substitution and charge on the component molecules was investigated and confirmed in a series of fully optimized calculations at the MP2/6-31+G(d) level. A proof-of-concept experiment to prepare a co-crystal between a prototypical ketone and a primary amine yielded the crystal structure reported herein, in which the hydrogen bonds between the co-crystal components indeed exhibit exclusively the designed and sought-after $R^2_4(8)$ motif.

Keywords: computational energetics · crystal engineering · graph sets · hydrogen bonds · supramolecular chemistry

Introduction

> “This work involves the use of crystal chemistry and crystallographic data base analyses as a way to study hydrogen-bond directed molecular recognition properties of organic molecules… The point of view taken here is to analyze the consequences of directed and selective hydrogen-bond interactions on sets of molecules rather than focusing on the energy or geometry of individual hydrogen-bond interactions. The “consequences” are to a solid-state chemist what a new synthesis is to a solution chemist, that is, the formation of a new chemical species.[1]”

Taken from the abstract of the late Margaret Etter’s landmark review article entitled “Hydrogen Bonds and Design Elements in Organic Chemistry”, these three sentences succinctly summarize much of the philosophy and strategy behind current efforts in crystal engineering of organic materials[2] and the design and preparation of co-crystals.[3] Etter also considerably aided in the recognition of “selective hydrogen-bond interactions in sets of molecules” by developing the use of graph sets to conveniently recognize and characterize the hydrogen-bond (and other) motifs,[4,5] many of which subsequently have also become known as synthons in the parlance of crystal engineering.[6] The main difference between patterns and synthons is in their use: motifs and the graph set notation to describe them were initially developed to analyze the structure of existing crystal structures, while the synthon concept (originally developed in connection with molecular synthesis by Corey[7]) is used to define building blocks in crystal engineering. Clearly the only motifs observed in crystals and the only synthons expected to exist in new crystals are those that are sufficiently robust to predominate in competition with other possible motifs (as local or global minima in the energy landscape of all possible motifs). Therefore, a rational design employing motifs is possible only after demonstrating the energetic robustness of the new motif of interest. That robustness could originate in thermodynamic factors, that is, the motif of interest is the most stable one, or from kinetic factors, that is, there are less stable (i.e., metastable) motifs, but the energetic pathways towards their realization involve energetic

---

[a] Prof. J. Bernstein
Department of Chemistry, Ben-Gurion University of the Negev
Beer Sheva, 84105 (Israel)
Fax: (+972) 8-529-0582
E-mail: yoel@bgu.ac.il

[b] Prof. J. J. Novoa
Departament de Química Física & IQTCUB, Facultat de Química
Universitat de Barcelona, Av. Diagonal
647, 08028-Barcelona (Spain)

[c] Prof. R. Boese, Dr. S. A. Cirkel
FB8/Anorganische Chemie, Universität Duisburg-Essen
Universitätstrasse 5, Essen (Germany) 45117 (Germany)

barriers with a higher energy than the available thermal energy. A metastable motif can be formed due to the interactions with the solvent or other species in the nucleation stage or in the early stages of crystal growth, or due to the formation in these early stages of lower symmetry aggregates in which the energy scale of the motifs is different; once formed, the crystal grows preserving these metastable motifs due to the kinetic factors indicated herein. A simple qualitative approach to gain control over the formation of the appropriate motifs takes advantage of combining the appropriate hydrogen bonds, the strongest and most directional intermolecular interactions, and then evaluating the stability of the resulting supramolecular aggregate that is obtained after the motif is formed by ab initio optimization.

We can now explore how to use these ideas for a rational design of co-crystals based on robust motifs. In essence, the formation of co-crystals is analogous to a chemical reaction. Two (or more) different reagents, say A and B, are 'reacted' to form a new product, say C. The reaction may take place in solution or simply by grinding together two solids.[8] By definition the desired product is the crystalline product C, so that the reaction mixture is commonly recrystallized to purify the product and/or to obtain crystals suitable for structure determination. The recrystallization procedure of C is the antithesis of one of the traditional methods of purification, since the desired result contains two or more components in a fixed stoichiometric ratio and structure rather than a single component. One working assumption is that the desired co-crystal is less soluble than any of the individual components. Since co-crystal formation does not result in the formation of new covalent bonds, the interactions between A and B involve only intermolecular forces, which are much weaker than covalent forces. However, the $A + B \rightarrow C$ transformation can still be considered from all points of view as a chemical reaction, or more specifically, as a supramolecular chemical reaction. Thus, we can extrapolate all of the theoretical concepts already developed for covalent chemical reactions into the supramolecular chemical reactions (potential energy surfaces, transition states, activation energies, minimum energy pathways, etc.).

We can focus on examples of motifs that could serve for the rational design of co-crystals. Much of the utilization of the use of hydrogen bonds for the design and preparation of co-crystals has revolved around the familiar $R^2_2(8)$ motif (Scheme 1). The $R^2_4(8)$ motifs result from the aggregation of four molecules to form a supramolecular aggregate in which the four D−H···A hydrogen bonds formed present the $R^2_4(8)$ topology, as in Scheme 1, a ring of eight atoms and four intermolecular A−H···B hydrogen bonds, involving four donor groups (D−H) and two acceptor groups (A), so that each of the acceptors is involved in two hydrogen bonds. The four molecules do not necessarily have to be different, but a case of particular interest for co-crystal design and synthesis is found when the donor A group is found in one class of molecules, whereas the acceptor group is found in the other class. We have earlier noted that the versatility of this motif was demonstrated in a survey of the Cambridge Structural Database (CSD), which indicated that at least 80 different functional groups can form such a motif.[9] Etter also recognized the tendency for nitroanilines to form the $R^2_1(4)$ motif, and used this information in attempting to prepare noncentrosymmetric crystals,[10] for instance, for use as nonlinear optical materials.

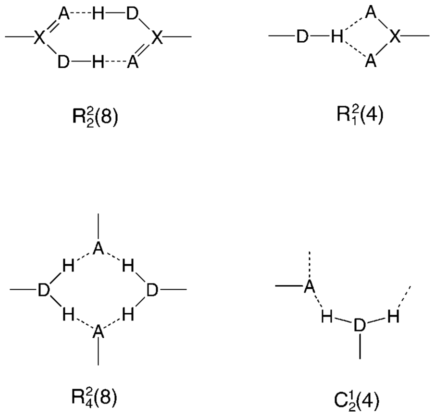

Scheme 1. Different types of hydrogen-bond motifs. A = hydrogen-bond acceptor, D = hydrogen-bond donor, X = any atom with the valency appropriate for the bonding shown.

The third pattern in Scheme 1 is the $R^2_4(8)$ motif, a potentially even more versatile motif, particularly for the controlled design and synthesis of co-crystals. We first recognized this motif in our early graph set analysis of iminodiacetic acid,[11] and later discussed its pervasiveness in a variety of chemical structures,[5] for instance, in a series of nitroanilines with triphenylphosphine or triphenylarsine oxides.[10a] A preliminary (and continuing) survey of the CSD has already identified over 12000 instances of this heteromotif, most of which contain four individual and unconnected molecules and/or ions.[12] A number of these cases involve two chemically different moieties (so that the motif itself containing four molecules is crystallographically centrosymmetric or pseudo-centrosymmetric). The widespread presence of the $R^2_4(8)$ motif in a variety of crystal-packing environments suggests that it is a sufficiently robust entity to be considered as a packing motif in the design of co-crystals. However, perhaps the most remarkable feature about this heteromotif in terms of possible co-crystal formation is that it potentially involves the intermolecular recognition and synthesis of a supramolecular entity comprised of four different molecules, a rare occurrence.[12,13] Consequently, such a driving force for molecular recognition could therefore be used to create co-crystals of up to four different chemical moieties.

However, for the functional groups involved in the cyclic $R^2_4(8)$ pattern there is at least one commonly encountered alternative motif. The combination of a functional group containing two hydrogen-bond donors with an acceptor that has two lone pairs can also lead to the chain motif $C^1_2(4)$. The realization of both the $R^2_4(8)$ and $C^1_2(4)$ motifs under different circumstances would lead to a polymorphic system. This is an example of a bond-making/-breaking process, that is, a supramolecular chemical reaction in which the $R_4^2(8)$ synthon is not formed, although the appropriate chemical functionality is present. Therefore, we have to understand the thermodynamic and kinetic factors that control the $R_4^2(8) \rightleftarrows C_2^1(4)$ supramolecular competition if we want to preserve the $R_4^2(8)$ synthon.

The ultimate utility of any supramolecular synthon as a building block for crystals depends on two factors: 1) the stability of the synthon relative to its isolated molecular components and 2) its thermodynamic and kinetic stability against its transformation into other possible motifs (by reordering of the hydrogen bonds that comprise the motif). Both factors depend on the properties of the hydrogen bonds that constitute the $R_4^2(8)$ motif and those resulting from it by all thermodynamic and kinetically allowed supramolecular reactions. This report deals with both of these factors for the case of the $R_4^2(8)$ motif in a wide variety of model complexes in which this motif is present. Thus, by carrying out ab initio calculations on molecular aggregates that contain the hydrogen-bond functionality appropriate for the potential formation of the $R_4^2(8)$ motifs, we will examine the thermodynamic stability of the $R_4^2(8)$ motif, as defined above, and the geometric parameters that it presents. These results can serve as guidelines in the generation of stable co-crystals presenting $R_4^2(8)$ motifs, for instance, for the choice of suitable co-crystal formers for a particular molecule. Utilizing the results of these calculations, we then describe a proof-of-concept experiment exploiting this motif for in Etter's words, "the formation of a new chemical species"—in this case the design and preparation of a prototypical co-crystal dominated by a $R_4^2(8)$ motif.

Stability and energetics of the $R_4^2(8)$ motif: The thermodynamic stability of the motif can be equated to the stability of the aggregate in comparison with its dissociation into four isolated molecules. To a first approximation, the thermodynamic stability of the $R_4^2(8)$ motif in a supramolecular aggregate can be obtained by summing the interaction energy of the four A−H···B hydrogen bonds formed. Note that in ring motifs it is well known that the strength of the hydrogen bonds is increased relative to that found in isolated dimers by cooperative effects.[14] It is worth noting that the motif can be thermodynamically stable (its energy is lower than the dissociated products), but not be kinetically stable (i.e., there is no barrier towards the transformation into a more stable motif). It is also worth pointing out that in many of the $R_4^2(8)$-containing aggregates studied herein, in addition to the four primary D−H···A hydrogen bonds defined in the initial model, in the computationally optimized geometry there are secondary motifs in the structure of the resulting supramolecular aggregate. These secondary motifs increase the thermodynamic and kinetic stability of the supramolecular aggregate, although the H···A distances involved suggest that they are weaker than the $R_4^2(8)$ motif. By looking at strength–length correlations, it would be possible to estimate the contribution of each of the D−H···A hydrogen bonds present in these secondary motifs. However, as noted above, a cooperative effect takes place when the strength of the central $R_4^2(8)$ motif may be increased by atoms in the motif connected to nearby hydrogen bonds. Given this situation, the possibility of these secondary motifs should also be considered as contributing to the $R_4^2(8)$ motif stability.

A first test of the robustness of the $R_4^2(8)$ motif to fragmentation, or transformation into another motif can be obtained by fully optimizing at the MP2/6-31+G(d) level the geometry of a variety of supramolecular aggregates of the $R_4^2(8)$ motif (see Scheme 2). The supramolecular aggregates were selected to systematically test the effect induced by the most common substituents on the motif structure and stability. The optimization was initiated by manually generating a $R_4^2(8)$ supramolecular aggregate in which the metrics of the four D−H···A hydrogen bonds involved closely approximate those found in dimers.[15] Then a first optimization of the geometry was carried out at the Hartree–Fock (HF) level, using the 6-31G(d) basis set. If the $R_4^2(8)$ motif was preserved in the HF optimized structure, then an MP2/6-31G(d) optimization was performed on the final HF/6-31G(d) optimized geometry. The MP2 method is known to provide good results for the computation of optimum geometries and interaction energies in hydrogen-bonded dimeric aggregates.[16]

We have found that in most of the aggregates studied herein the initial $R_4^2(8)$ motif was preserved in the final MP2/6-31G(d) optimum geometry. However, in some cases (indicated in Scheme 2), during the course of the optimization the starting $R_4^2(8)$ motif transforms into a more stable one, by reordering the hydrogen bonds from the initial model to those generated in the course of the optimization. The presence of the $R_4^2(8)$ motif in the initial structure, or during any of the steps of the geometry optimization was determined by examining the hydrogen bonds formed within the aggregate. The existence of the hydrogen bonds and the topology required for a $R_4^2(8)$ motif was confirmed by analyzing the D−H···A distances and angles for the shortest of these interactions requiring that they must lie within the ranges of angles and distances reported in the literature for the specific hydrogen bond analyzed.[17]

All geometry optimizations and energy evaluations were carried out by using the appropriate options in Gaussian 03.[18] No correction was made for the basis set superposition error (BSSE),[19] since 1) our interest in the interaction energies is essentially qualitative (sign and relative order of magnitude of the interaction energy), and 2) previous studies on dimers indicate that the usual methods employed to correct the BSSE (the counterpoise method) overestimate the MP2/6-31G(d) BSSE error.[20]

Results of energy calculations

Comparison with the $R_2^2(8)$ motif: Since the energetics of the $R_4^2(8)$ motif has not been studied previously, it was necessary first to establish an energetic frame of reference for the set

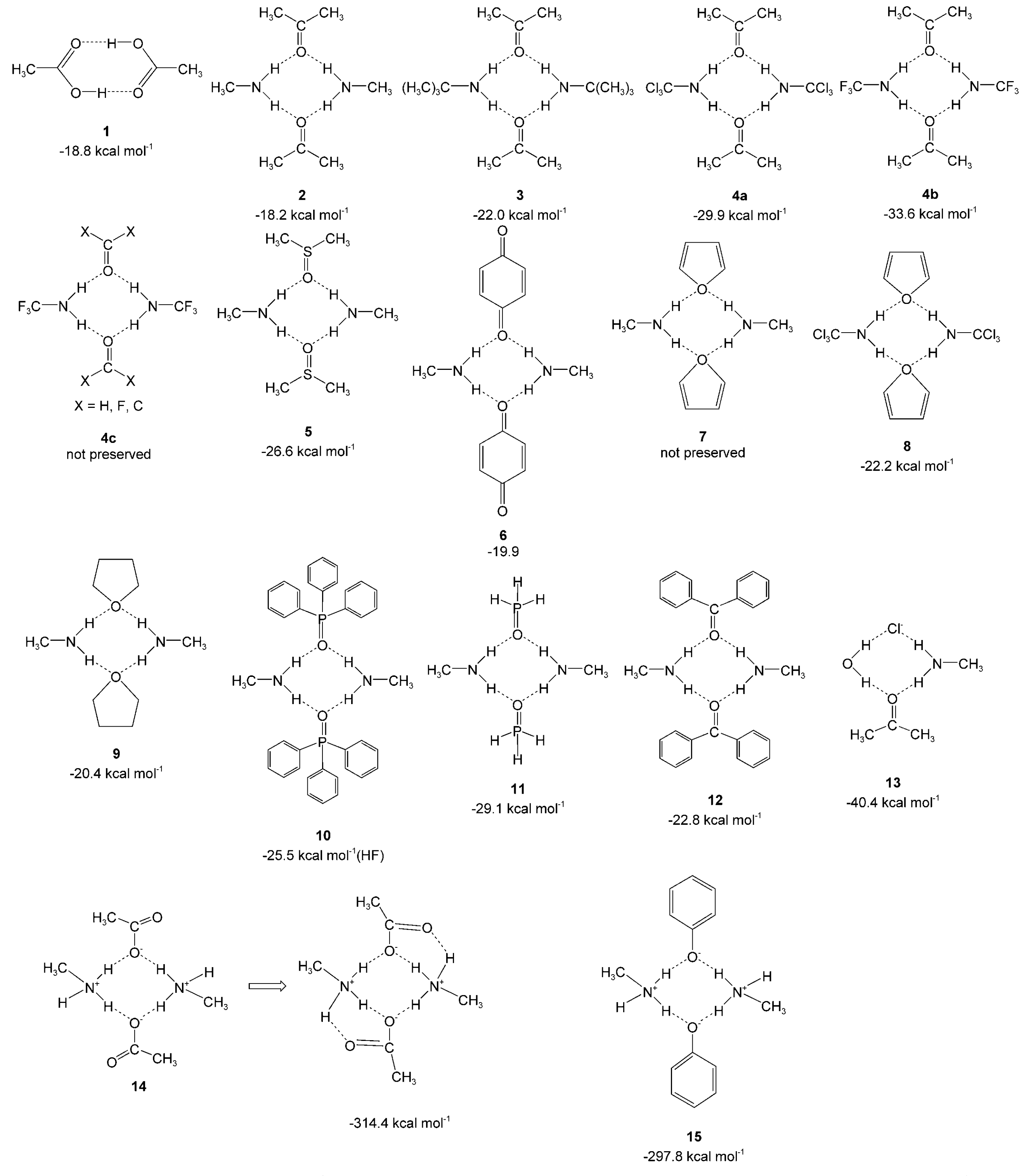

Scheme 2. Examples of aggregates presenting $R_4^2(8)$ motifs (under each structure, its identification number and interaction energy, in kcal mol^{-1}, is given) used to study the stability of such motif by doing an MP2 geometry optimization using a 6-31G(d) basis set. HF after the interaction energy indicates that the HF method was used, due to the size of the system. A negative interaction energy indicates that the aggregate is stable against its dissociation into the four constituent fragments. When the motif is not preserved during the optimization, this is explicitly indicated under the structure number.

of calculations. For this we chose the prototypical $R_2^2(8)$ motif found in the acetic acid dimer **1**. As shown in Scheme 2, the stabilization energy for the $R_2^2(8)$ motif in **1** is 18.8 kcal mol^{-1}, or 9.4 kcal mol^{-1} per hydrogen bond, that is, almost twice the stabilization energy of a O−H···O hydrogen bond in an isolated water dimer[21] (all energies in Scheme 2 are interaction energies, and a negative sign indicates that the aggregate is stable with regard to its dissociation into its constituents fragments). The 18.8 kcal mol^{-1} stabilization energy originates from a BSSE uncorrected interaction energy (of -18.8 kcal mol^{-1}), and following the BSSE correction using the counterpoise method[19,20] becomes 13.8 kcal mol^{-1}. As it is well known that the BSSE method overcorrects when using the 6-31G(d) basis set, the interaction energy was also computed by using a much better basis set, the aug-cc-pVTZ.[22] The MP2 BSSE uncorrected and corrected stabilization energy obtained with this basis are 17.5 and 16.2 kcal mol^{-1}, respectively, that is, values very close to the uncorrected ones obtained at the MP2/6-31G(d) level. As we will demonstrate below, the $R_2^2(8)$ and $R_4^2(8)$ motifs fall in the same range of energy values.

Robustness of the $R_4^2(8)$ motif: Scheme 2 shows all of the initial geometries of the supramolecular aggregates used to test the robustness of the $R_4^2(8)$ motifs in a schematic form. In the cases for which the motif was preserved during the full geometry optimization, its dissociation energy (into four fragments at their optimum geometry) is indicated. In a few cases, the motif was not preserved during the optimization, and this fact is also indicated in Scheme 2. The optimized geometry for each of the supramolecular aggregates of Scheme 2 is plotted in Figure 1 1) to allow the determination of the primary and secondary hydrogen bonds that participate in the $R_4^2(8)$ stability, and 2) to indicate the transformations undergone by these motifs in those cases that resulted in the collapse of the original motif. The most relevant geometrical parameters of the optimum geometry are also collected in Table 1 in the Supporting Information. The ultimate value of these results is to serve as guidelines for the selection of suitable candidates to form co-crystals based on this motif as one of the design features.

The molecular moiety that acts as an acceptor in the $R_4^2(8)$ motif is characterized by a pair of orbitals with nonbonding electrons. For the examples described to this point those orbitals were on an oxygen atom with formal sp^2 hybridization. In principle, an oxygen with formal sp^3 hybridization can also serve as an acceptor for two hydrogen bonds, but as H·M.>·O(sp^3) hydrogen bonds are generally weaker than H···O(sp^2),[23,24] we decided to start our test computations with an oxygen atom with formal sp^2 hybridization. The archetypical example of $R_4^2(8)$ motif is that generated from methylamine and acetone **2**. The MP2/6-31G(d) computed stabilization energy is 18.2 or 4.5 kcal mol^{-1} per hydrogen bond. The MP2/6-31G(d) BSSE corrected stabilization energy using the four-body counterpoise correction is 8.3 kcal mol^{-1}. When the calculation was performed at the more accurate MP2/aug-cc-pVTZ level, the BSSE-uncorrected and -corrected stabilization energies were 15.7 and 13.2 kcal mol^{-1}, respectively, both in the range of the BSSE-uncorrected results; consequently, we concluded that the MP2/6-31G(d) BSSE-uncorrected values were sufficiently close to the MP2/aug-cc-pVTZ BSSE-corrected and -uncorrected energies to give results sufficiently accurate for the comparisons we intended to make herein. The previous numbers show that the $R_4^2(8)$ and $R_2^2(8)$ motifs present a similar stabilization energy, and that such similarity is well reproduced by the BSSE-uncorrected results. Therefore, as in the rest of this work, we intended to examine relative changes of the stabilization energy for complexes in which the main $R_4^2(8)$ motifs is preserved, we evaluate these changes at the MP2/6-31G(d) level, expecting that the BSSE error is always similar to the previously estimated one. Note also that each individual hydrogen bond participating in the $R_4^2(8)$ motif is weaker than those normally observed in say, amide structures,[25] and that the H···O distances are also longer in the $R_4^2(8)$ motifs. Figure 1 shows that, besides the primary $R_4^2(8)$ motif, two secondary $R_2^2(6)$ motifs are present (which involve one of the N−H···O bonds that participate in the $R_4^2(8)$ motif, and a C−H···N bond, the H···N distance of which is 2.518 Å).

The replacement of methylamine with *tert*-butylamine in **3**, which increases the electronegativity of the nitrogen and the donor ability of the amino hydrogen atoms, led to an optimum geometry for the aggregate with a principal $R_4^2(8)$ motif, but now complemented by two secondary $R_2^1(6)$ motifs (involving a new C−H···O bond, with a H···O distance of 2.695 Å). The additional stabilization in **3** over **2** is 4 kcal mol^{-1} (total 22.2 kcal mol^{-1}) or $\approx$1 kcal mol^{-1} per hydrogen bond, which in part reveals the effect of the secondary motif. This aggregate stability may be enhanced by substituting all of the hydrogen atoms on the methyl group in methylamine by chlorine or fluorine as in **4a** and **4b**. In both cases, two $R_2^2(6)$ secondary motifs are present, and the extra stability should be better than that found in **2**. The resulting interaction energy in **4a** (-29.9 kcal mol^{-1}) is an additional stabilization of nearly 2 kcal mol^{-1} per hydrogen bond relative to that in **3**. In **4b** the interaction energy (-33.6 kcal mol^{-1}) represents an additional stabilization energy relative to **3** of nearly 3 kcal mol^{-1}.

When the hydrogen atoms of the acetone molecules in **2** are replaced by F or Cl groups, as in **4c**, the $R_4^2(8)$ motif present in **2** is not preserved. However, replacing the acetone acceptor in the archetypal $R_4^2(8)$ motif present in **2** with a better acceptor, that is, dimethylsulfoxide **5**, leads to an additional stabilization of $\approx$8 kcal mol^{-1} over prototype **2**. Not surprisingly, benzoquinone as an acceptor of two hydrogen bonds **6** does not lead to a significant stabilization over acetone, since there is no significant source of additional electron density in the lone pairs on the carbonyl oxygen.

Indeed, a water molecule serves as an acceptor for two hydrogen bonds in many examples of $R_4^2(8)$ in the CSD[12,26]. An ethereal oxygen may potentially act in the same capacity. Hence, we examined the $R_4^2(8)$ tetramer between methylamine and furan **7**. Upon minimization, this tetramer goes through a very shallow minimum before progressing to a more stable tetramer that contains two (furan) C−H···N hydrogen bonds, due to the acidity of the furan hydrogen atoms. That is, the $R_4^2(8)$ motif collapses to $R_3^3(7)$ motifs. The replacement of the methyl group on the amine with $-CCl_3$ as in **8** can increase the electronegativity of the nitrogen and thus the strength of the (amine)N−H···O(furan) hydrogen bond, potentially overcoming the tendency to form

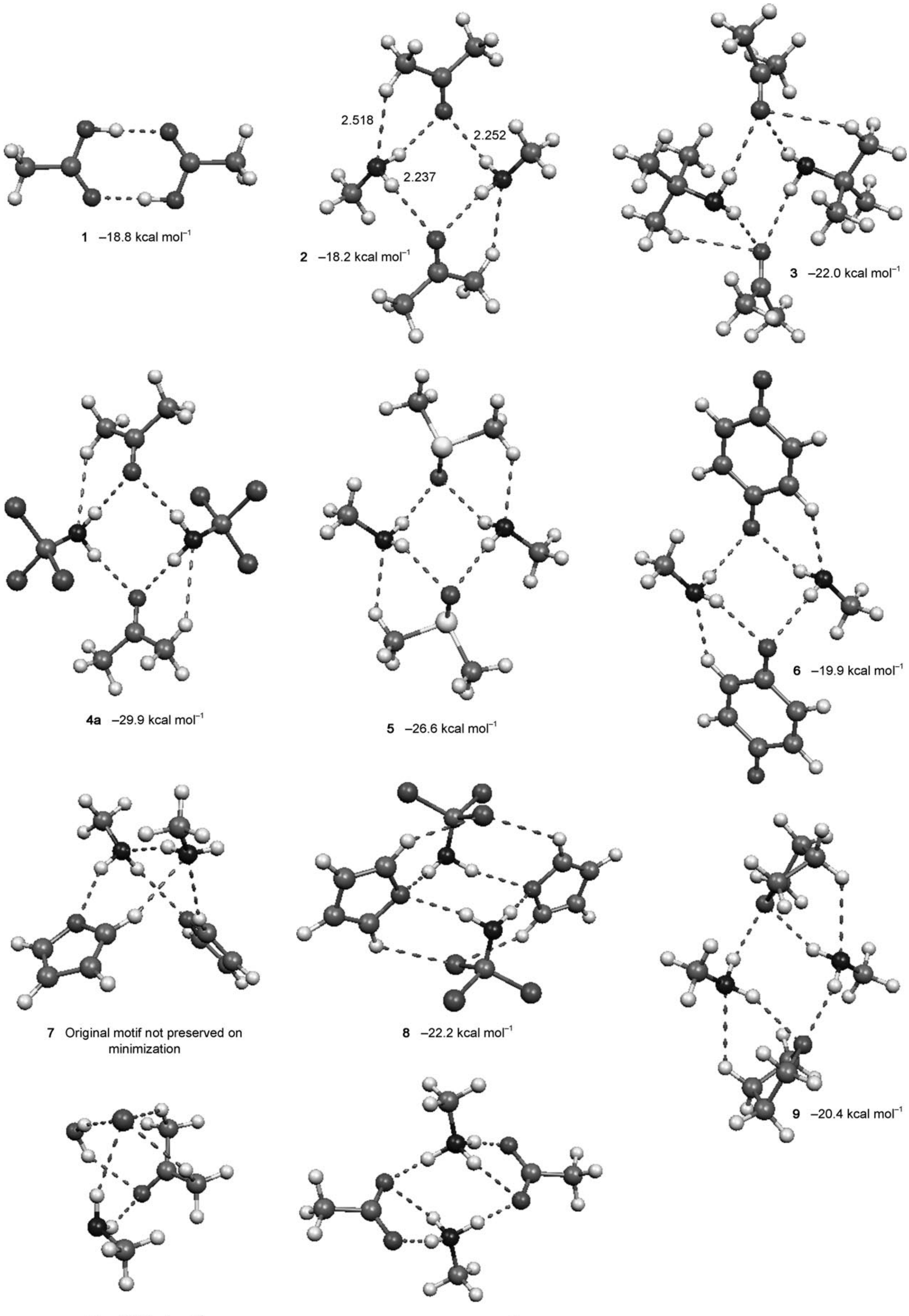

1 −18.8 kcal mol^{-1}

2 −18.2 kcal mol^{-1}

3 −22.0 kcal mol^{-1}

4a −29.9 kcal mol^{-1}

5 −26.6 kcal mol^{-1}

6 −19.9 kcal mol^{-1}

7 Original motif not preserved on minimization

8 −22.2 kcal mol^{-1}

9 −20.4 kcal mol^{-1}

13 −40.4 kcal mol^{-1}

14 −314.4 kcal mol^{-1}

Figure 1. Optimum geometry of the most relevant $R_4^2(8)$ aggregates of Scheme 2.

the (furan)C–H···N hydrogen bond. Indeed, the resulting $R_4^2(8)$ tetramer has a stability essentially identical to that of the *tert*-butylamine/acetone derivative, although a short intramolecular C–H···Cl distance results. Notice that in **8**, besides the primary $R_4^2(8)$ motif, the aggregate contains four $R_2^2(7)$ motifs involving C(sp^2)–H···Cl hydrogen bonds. On the other hand, reducing the acidity of the furan hydrogen atoms by using tetrahydrofuran leads to a motif **9** with an energy of stabilization of 20 kcal mol^{-1}, that is, 2 kcal mol^{-1} weaker than that of **8**. It is also worth pointing out that the secondary motifs in **9** ($R_2^2(6)$, involving C–H···N bonds) are different from those in **8**.

Substituting acetone by the more basic $X_3P{=}O$ ($X = C_6H_5$, H) molecules was also evaluated in aggregates **10** and **11**. Their stability is increased relative to that of **2** by 7.3 and 10.9 kcal mol^{-1}, thus indicating a clear effect of the basic group on the strength of the $R_4^2(8)$ motif. The same effect can be tested by comparing the stabilization of **2** with the case in which the methyl groups of the two acetone molecules has been replaced by phenyl groups (i.e., benzophenone replacing acetone) as in **12**, the stabilization of which is −22.8 kcal mol^{-1}.

All of the tetramers examined to this point contained only neutral molecules. Clearly one or more of the moieties can also be charged, leading either to a charged, or ionic but neutral, tetramer. We examined the effect of a single charged entity by carrying out the calculation on a tetramer containing methylamine and water as the two biprotonic donors and acetone and a chloride ion as the two acceptors for two hydrogen bonds, **13**. This tetramer, of course, will formally bear a single negative charge, located essentially on the chloride ion. The stabilization is significantly increased to 40.38 kcal mol^{-1}, although the motif is severely distorted upon energy minimization resulting in two secondary $R_3^2(8)$ motifs (involving the C–H···Cl$^-$ bonds). The additional stability of **13** relative to all other previously described neutral aggregates is due to the higher strength of the A–H···B$^-$ charge-assisted hydrogen bonds with respect to the A–H···B neutral hydrogen bonds.

A measure of the stabilization was obtained when two charges of opposite sign are present in the aggregate when examining the tetramer of two methylammonium cations and two acetate anions, **14**. The "pure" $R_4^2(8)$ tetramer starting model minimizes to a tetramer in which the motif is still present, but the molecules are reoriented to allow the formation of two additional (and longer H···O distance of 2.346 Å) N–H$^{(+)}$···O$^{(-)}$ hydrogen bonds that form a $R_2^2(6)$ motif. The $R_4^2(8)$ motif in this case has four N–H$^{(+)}$···O$^{(-)}$ bonds with a H···O distance of 1.608 Å. All these N$^{(+)}$–H···O$^{(-)}$ bonds, involving fragments with a net charge of opposite sign, are an example of an ion–ion hydrogen bond, which have been found to exhibit strengths well above the covalent limit (50 kcal mol^{-1}) previously presumed to be the largest possible hydrogen bond.[26] Not unexpectedly, the stabilization energy for the motif increases by approximately an order of magnitude to 314.37 kcal mol^{-1}. We also studied aggregate **15** to test the effect of using different anions. The results indicated that the interaction energy of the two aggregates is similar, as one would expect given the Coulombic nature of the interaction between ions in the two cases (our calculations indicate that the dominant term, q_1q_2/r_{12}, depends on the net charge placed on the two fragments and their intermolecular distance more than in general on the exact distribution of the net atomic charges over the atoms, that is the chemical structure of the fragments).

Proof-of-concept experiment: If the $R_4^2(8)$ motif is to serve as a supramolecular synthon—a synthetically useful means toward achieving co-crystals by design—then as for any other reagent in chemical synthesis, its potential and its limits must be determined. The first step in this process is the demonstration that it indeed is a synthetic tool, and that crystals containing this motif can be prepared by design. As in much of chemistry, the proof-of-concept experiment often involves the choice of the simplest prototypical system to demonstrate directly the concept or the model in question, while eliminating as many other potentially complicating variables as possible.

For the experiment on the neutral $R_4^2(8)$ tetramer we chose acetone as the simplest possible carbonyl to provide the two accepting sites, while avoiding the hydrogen-bonding-donor potential of, say, the hydrogen of an aldehyde. For the prototype hydrogen-bond donor we chose methylamine with only two possible hydrogen bond donors, which would lead to the co-crystal **2**. At room temperature acetone is a liquid and methylamine is a gas. Hence, special techniques are required to carry out the attempted co-crystallization of these two components.[28]

Attempts to obtain a co-crystal of acetone and methylamine so far have been unsuccessful. We did obtain two of the three known polymorphs of acetone,[29] and experiments to obtain the co-crystal are continuing. As the failure suggests a preference for each component to pack with like molecules, we thought that hydrogen bonding could be promoted by steric protection of the N lone pairs, by increasing the size of the alkyl group on the amine. A number of alkyl amines were studied, and the first co-crystal was obtained with acetone and *tert*-butylamine in a 1:1 mixture by volume. The triclinic crystal contains a 3:1 molar ratio of *tert*-butylamine and acetone, but in the desired $R_4^2(8)$ centrosymmetric tetramer **3** as a packing motif as indicated by N–H···O hydrogen bonds, indicated by light blue and yellow dotted lines (Figure 2, distances are given in the figure caption). Since the amine nitrogen atoms (N3, N3′) involved in the $R_4^2(8)$ motif are not only double proton donors, but also single proton acceptors, they are saturated at the rear by further amine protons (from N2, N2′, green dotted lines), which are again linked to further *tert*-butylamine molecules (N1, N1′, pink dotted lines)). Both the attached amine molecules are involved in C(methyl)–H···N interaction (not shown for clarity).

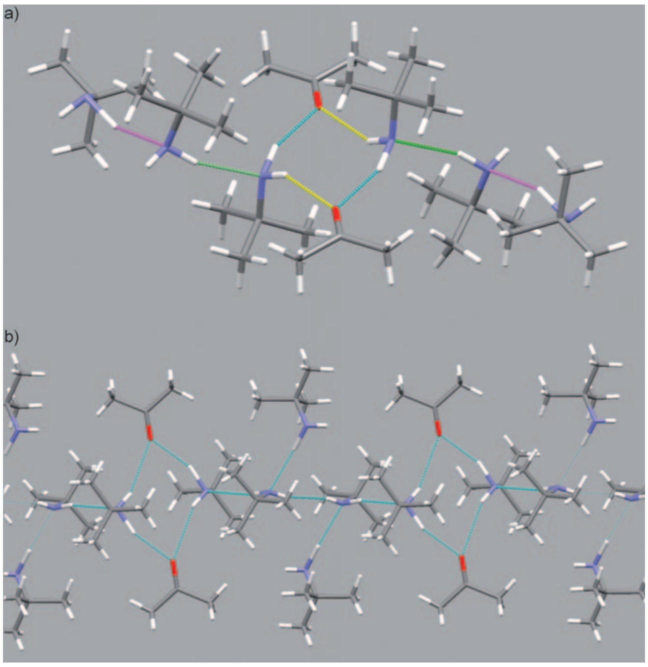

Figure 2. a) The $R_4^2(8)$ hydrogen-bond motif in the crystal structure of the co-crystal of *tert*-butylamine/acetone (3:1) is shown in the center. The N···O distances are 3.277 Å (light blue) and 3.317 Å (yellow), respectively. The external hydrogen bond N3···N2 is 3.240 Å (green) and N2···N1 is 3.277 Å (pink). b) View of the crystal packing [011] of the 3:1 *tert*-butylamine/acetone co-crystal shows the hydrogen-bonded systems with the $R_4^2(8)$motifs and the peripherally arranged methyl groups that separate the chains.

Conclusion

This study has demonstrated the potential for developing a strategy for designing and preparing co-crystals on the basis of the structural and energetic principles that regulate the geometry and the relative stability of specific hydrogen-bonding motifs. Both sets of data are obtained from ab initio MP2 geometry optimizations of aggregates presenting the motif of interest. Analogous to the development of synthetic methods for making and breaking chemical bonds, the object is not to provide foolproof methods for obtaining co-crystals, but rather to aid in choosing appropriate reagents for attempting the co-crystallization of a specific molecule with particular functional groups—in this case an atom containing two potential hydrogen-bond donors and another with two electron lone pairs.

The proof-of-concept experiment reported herein indicates the viability of such an approach. The use of appropriate calculations can aid in the design strategy prior to undertaking experiments. Some of our additional attempts to employ this strategy have led to co-crystals between benzidine as a donor and benzoquinone, triphenhylphosphine oxide, and dimethyl sulfoxide as acceptors have yielded co-crystals, although none have exhibited the $R_4^2(8)$ motif.[29b] However, the last of them is in fact a hydrate in which water of solvation forms an $R_4^2(8)$ motif with both the donor and the acceptor molecules, suggesting that the $R_4^2(8)$ motif might be obtained in crystals prepared under anhydrous conditions. Furthermore, the strategy described herein did lead to a co-crystal of γ-aminobutanoic acid (GABA) and benzoic acid with the $R_4^2(8)$ motif.[29a] Other experiments incorporating ionic molecular species generated by varying the pH have led to co-crystals exhibiting the $R_4^2(8)$ motif in more than half of the crystals prepared.[12]

Finally, this investigation has also demonstrated that the use of the CSD to provide information on the occurrence and metrics of potential motifs for co-crystal formation, together with suitable computational studies to investigate the energy landscape of the motif is a viable method for developing strategies for the preparation of co-crystals.

Experimental Section

Experimental X-ray data: A 0.3 mm diameter quartz capillary was filled with *tert*-butylamine and acetone in a 1:1 ratio and flame-sealed. Mounted at a Bruker SMART/Apex2 diffractometer ($\mathrm{Mo}_{K\alpha}$ radiation), the capillary was cooled to 163 K and a bunch of poorly diffracting single crystals were grown from the polycrystalline material by means of the OHCD system applying a computer controlled miniature zone refining procedure, heated with an IR laser.[28] Formula $3(C_4H_{11}N)\cdot C_3H_6O$; formula weight 277.49 Da; space group $P\bar{1}$; $\rho = 0.909\ \mathrm{g\,cm^{-3}}$; cell dimensions $a = 9.6000(9)$, $b = 11.072(9)$, $c = 11.621(10)$ Å; $\alpha = 98.97(2)$, $\beta = 112.07(2)$, $\gamma = 110.22(2)°$; $V = 823.1(2)$ Å^3; $Z = 2$; 3311 independent ($R_{\mathrm{merg}} = 0.082$) and 1278 observed reflections ($2\theta_{\max} = 56.46°$); structure solved with direct methods and refined with Bruker SHELXTL-Plus program Vers. 2008/4. The amine hydrogen atoms were riding on the N atoms at the positions located in a difference Fourier with free isotropic U values, methyl H atoms in calculated positions, riding on the C atoms with the 1.5-fold isotropic U values of the corresponding C atoms. 179 parameters, $R1 = 0.1202$, $wR2 = 0.3310$, max residual electron density $0.48\ \mathrm{e\,Å^{-3}}$. CCDC-709941 contains the supplementary crystallographic data for this paper. These data can be obtained free of charge from the Cambridge Crystallographic Data Centre via www.ccdc.cam.ac.uk/data_request/cif.

Acknowledgements

This work was supported in part by the United States—Israel Binational Science Foundation (BSF) grant no. 2004118, the Spanish Science and Education Ministry (projects BQU2002-04587-C02-02 and UNBA05-33-001) and the Catalan CIRIT (projects 2001SGR-0044 and 2005-PEIR-0051/69). R.B. and S.A.C. acknowledge support from the DFG-Forschergruppe 618. Computer time was also provided by CESCA and BSC. J.B. and J.J.N. also wish to thank HPC-Europa for a fellowship to support the computational work reported here and for a stay by J.B. at the Barcelona Supercomputer Center.

---

[1] M. C. Etter, *J. Phys. Chem.* **1991**, *95*, 4601–4610.

[2] a) G. R. Desiraju in *Crystal Design: Structure and Function*, Wiley, Toronto **2003**; b) D. Braga, F. Grepioni, *Chem. Commun.* **2005**, 3635–3645.

[3] a) Ö. Almarsson, M. J. Zaworotko, *Chem. Commun.* **2004**, 1889–1896; b) C. B. Aakeröy, A. M. Beatty, B. A. Helfrich, *Angew. Chem.* **2001**, *113*, 3340–3346; *Angew. Chem. Int. Ed.* **2001**, *40*, 3240–3246.

[4] a) M. C. Etter, *Acc. Chem. Res.* **1990**, *23*, 120–126; b) M. C. Etter, J. C. Macdonald, J. Bernstein, *Acta Crystallogr. Sect. B.* **1990**, *46*, 256–262.

[5] J. Bernstein, R. E. Davis, L. Shimoni, N.-L. Chang, *Angew. Chem.* **1995**, *107*, 1689–1708; *Angew. Chem. Int. Ed. Engl.* **1995**, *34*, 1555–1573.

[6] G. R. Desiraju, *Angew. Chem.* **1995**, *107*, 2541–2558; *Angew. Chem. Int. Ed. Engl.* **1995**, *34*, 2311–2327.

[7] E. J. Corey, *Pure Appl. Chem.* **1967**, *14*, 19–37.

[8] a) N. Shan, F. Toda, W. Jones, *Chem. Commun.* **2002**, 2372–2373; b) A. V. Trask, W. D. S. Motherwell, W. Jones, *Chem. Commun.* **2004**, 890–891.

[9] a) R. E. Davies, J. Bernstein, *Trans. Am. Crystallogr. Assoc.* **1998**, *34*, 7–21.

[10] a) M. C. Etter, K. S. Huang, G. M. Frankenbach, D. A. Adsmond in *Materials for Nonlinear Optics - Chemical Perspectives ACS Symposium Series, Vol. 455* (Eds.: S. R. Marder, J. E. Sohn, G. Stucky), ACS, Washington, **1991**, pp. 446–456; b) K. S. Huang, D. Britton, M. C. Etter, S. R. Bryn, *J. Mater. Chem.* **1997**, *7*, 713–720.

[11] J. Bernstein, M. C. Etter, J. C. MacDonald, *J. Chem. Soc. Perkin Trans. 2* **1990**, 695–698.

[12] S. Eppel, J. Bernstein, *Acta Crystallogr. Sect. B* **2008**, *64*, 50–56.

[13] a) B. R. Bhogala, S. Basavoju, A. Nangia, *Cryst. Growth Des.* **2005**, *5*, 1683–1686; b) J. Bernstein, A. Eisenstein, S. Eppel, unpublished results.

[14] a) S. S. Xantheas, *J. Chem. Phys.* **1994**, *100*, 7523–7534; b) C. Lee, H. Chen, G. Fitzgerald, *J. Chem. Phys.* **1995**, *102*, 1266–1269; c) J. J. Novoa, F. Mota, R. D'Oria in *Hydrogen Bonding. New Insights* (Ed., S. J. Grabowski), Springer, Dordrecht, **2006**, Chapter 5.

[15] S. Scheiner in *Hydrogen Bonding. A Theoretical Perspective*, Oxford University Press, New York, **1997**.

[16] P. Hobza in *Weak Intermolecular Interactions in Chemistry and Biology*, Elsevier, Amsterdam, **1978**; see also reference [15].

[17] G. A. Jeffrey, W. Saenger in *Hydrogen Bonding in Biological Structure*, Springer, Berlin, **1991**.

[18] Gaussian 03, Revision C.02, M. J. Frisch, G. W. Trucks, H. B. Schlegel, G. E. Scuseria, M. A. Robb, J. R. Cheeseman, J. A. Montgomery, Jr., T. Vreven, K. N. Kudin, J. C. Burant, J. M. Millam, S. S. Iyengar, J. Tomasi, V. Barone, B. Mennucci, M. Cossi, G. Scalmani, N. Rega, G. A. Petersson, H. Nakatsuji, M. Hada, M. Ehara, K. Toyota, R. Fukuda, J. Hasegawa, M. Ishida, T. Nakajima, Y. Honda, O. Kitao, H. Nakai, M. Klene, X. Li, J. E. Knox, H. P. Hratchian, J. B. Cross, V. Bakken, C. Adamo, J. Jaramillo, R. Gomperts, R. E. Stratmann, O. Yazyev, A. J. Austin, R. Cammi, C. Pomelli, J. W. Ochterski, P. Y. Ayala, K. Morokuma, G. A. Voth, P. Salvador, J. J. Dannenberg, V. G. Zakrzewski, S. Dapprich, A. D. Daniels, M. C. Strain, O. Farkas, D. K. Malick, A. D. Rabuck, K. Raghavachari, J. B. Foresman, J. V. Ortiz, Q. Cui, A. G. Baboul, S. Clifford, J. Cioslowski, B. B. Stefanov, G. Liu, A. Liashenko, P. Piskorz, I. Komaromi, R. L. Martin, D. J. Fox, T. Keith, M. A. Al-Laham, C. Y. Peng, A. Nanayakkara, M. Challacombe, P. M. W. Gill, B. Johnson, W. Chen, M. W. Wong, C. Gonzalez, J. A. Pople, Gaussian, Inc., Wallingford CT, **2004**.

[19] S. F. Boys, F. Bernadi, *Mol. Phys.* **1970**, *19*, 553-566.

[20] J. J. Novoa, M. Planas, M.-H. Whangbo, *Chem. Phys. Lett.* **1994**, *225*, 240–246.

[21] D. Feller, *J. Chem. Phys.* **1992**, *96*, 6104–6114.

[22] D. E. Woon, T. H. Dumming, Jr., *J. Chem. Phys.* **1993**, *98*, 1358.

[23] For two examples, see: a) J. J. Novoa, B. Tarrón, M.-H. Whangbo, J. M. Williams, *J. Chem. Phys.* **1991**, *95*, 5179–5186; b) Y. Zhao, D. G. Truhlar, *J. Chem. Theory Comput.* **2006**, *2*, 1009–1016.

[24] J. J. Novoa, F. Mota, *Chem. Phys. Lett.* **1997**, *266*, 23–30.

[25] K. Kim, K. D. Jorgan, *J. Phys. Chem.* **1994**, *98*, 10089–10094.

[26] a) M. Wenger, J. Bernstein, *Angew. Chem.* **2006**, *118*, 8134–8137; *Angew. Chem. Int. Ed.* **2006**, *45*, 7966–7969; b) M. Rafilovich, J. Bernstein, M. B. Hickey, M. Tauber, *Cryst. Growth Des.* **2007**, *9*, 1777–1782.

[27] E. D'Oria, J. J. Novoa, unpublished results.

[28] R Boese, M. Nussbaummer in *Correlations, Transformation and Interaction in Organic Crystal Chemistry, Vol. 7* (Eds.: D. W. Jones, S. Katrusiak), Oxford University Press, Oxford, **1994**, pp. 20–37.

[29] a) D. R. Allan, S. J. Clark, R. M. Ibberson, S. Parsons, C. R. Pulham, L. Sawyer, *Chem. Commun.* **1999**, 751–752; b) J. C. Huffman, **2001**, private communication, CSD Refcode HIXHIF05.

Received: October 16, 2009
Revised: April 6, 2010